Bioorganic & Medicinal Chemistry Letters 23 (2013) 1846–1852

Contents lists available at SciVerse ScienceDirect

Bioorganic & Medicinal Chemistry Letters

journal homepage: www.elsevier.com/locate/bmcl

Synthesis and biological evaluation of new cytotoxic indazolo[4,3-*gh*]isoquinolinone derivatives

Manochehr Shahabi [a], Eva Schirmer [a], Karem Shanab [a], Theerachart Leepasert [a], Jana Ruzicka [a], Wolfgang Holzer [a], Helmut Spreitzer [a,*], Babette Aicher [b], Peter Schmidt [b], Lars Blumenstein [b], Gilbert Müller [b], Eckhard Günther [b]

[a] *Department of Drug and Natural Product Synthesis, University of Vienna, Althanstraße 14, 1090 Vienna, Austria*
[b] *AeternaZentaris GmbH, Weismuellerstrasse 50, 60314 Frankfurt, Germany*

ARTICLE INFO

Article history:
Received 28 September 2012
Revised 2 January 2013
Accepted 4 January 2013
Available online 23 January 2013

Keyword:
Anticancer compounds

ABSTRACT

A series of indazolo[4,3-*gh*]isoquinolinones derivatives have been synthesized to decrease cardiotoxic side effects in comparison to Mitoxantrone. The antiproliferative effects of different side chains were investigated and tested on at least four different cell lines of cervix, ovarian, CNS, NSCLC (non-small-cell lung cancer) and colon carcinoma. In addition to antiproliferative activities, influence on cell cycle and intercalation behavior have been tested.

Mitoxantrone is used for fighting a wide range of cancerous diseases.[1] Unfortunately, its applicability is strongly limited due to cardiotoxic adverse effects. The search for antitumor antibiotics led to Pixantrone which was developed to reduce heart damage related to treatment while retaining efficacy. Pixantrone (BBR 2778) is currently in phase III of clinical trials in patients with Non-Hodgkin's lymphoma.[2]

Based on the work of Krapcho et al.[3] we developed a series of new cytotoxic indazolo[4,3-*gh*]isoquinolinones to eliminate cardiotoxicity. The new derivatives, lacking hydroxy substitution and bearing a nitrogen atom in the anthrapyrazole chromophore, should be less susceptible to biological reduction to anionic radicals which are responsible for cardiotoxicity, as for inhibition of topoisomerase II enzyme.[4] A wider range of activity and reduced side effects were the aims of the reported study.

In this letter, we present another series of novel cytotoxic compounds with different side chains attached on the key structure shown in Figure 1.

As previously reported by the authors,[5–7] the position of the nitrogen(s) in annelated rings are also essential for cytotoxic activity. All of the synthesized indazolo[4,3-*gh*]isoquinolinones were tested for cytotoxicity against a panel of five cancer cell lines.

In addition to the antiproliferative effects, we also investigated DNA intercalation behavior and the influence on cell cycle arrest. Furthermore, data on metabolic stability, pH stability and physicochemical properties are reported. Docking studies are discussed to rationalize the observed cytotoxic activities.

We report the synthesis of 23 different N-substituted compounds (shown in Table 1) and their precursors derived from the key structure shown in Figure 1.

For the synthesis of the tetracyclic nucleus 11 commercially available 3-chloropyridine 2 was treated with lithium diisopropylamide (LDA) and carbon dioxide to give 3-chloroisonicotinic acid 3 which was converted into methyl ester 4 using diazomethane. The key step for this synthesis lies in the nickel mediated coupling of ester **4** and compound **7**. This organo zinc bromide **7** was prepared by treating **6** with zinc dust in tetrahydrofuran (THF). Benzylbromide **6** was obtained by reacting 5-fluoro-2-chlorotoluene **5** with *N*-bromosuccinimide (NBS) in carbon tetrachloride. The addition of a solution of **7** in THF to methyl ester **4** in the presence of bis[triphenylphosphine]nickel(II) chloride led to coupled product **8**. Basic hydrolysis of **8** afforded carboxylic acid **9**, which was cyclized and oxidized to **10** by fuming sulfuric acid. The incorporation of the pyrazole ring was accomplished by reacting **10** with *N*,*N*-dimethylethylhydrazine to give **11** in good yields (Scheme 1).

Compounds **12**–**17** were prepared by nucleophilic aromatic substitution of chlorine of precursor **11** with an appropriate commercially available amine (Scheme 2).

Aziridines **21**–**23** were prepared from mesylates **18**–**20**, which in turn were obtained by treatment of corresponding alcohols **41**–**43** with mesyl chloride/triethylamine. Alcohols **41**–**43** were synthesized by introducing the appropriate O-protected hydroxyl amine

* Corresponding author. Tel.: +43 1427755621; fax: +43 142779556.
E-mail address: helmut.spreitzer@univie.ac.at (H. Spreitzer).

0960-894X/$ - see front matter © 2013 Elsevier Ltd. All rights reserved.
http://dx.doi.org/10.1016/j.bmcl.2013.01.022

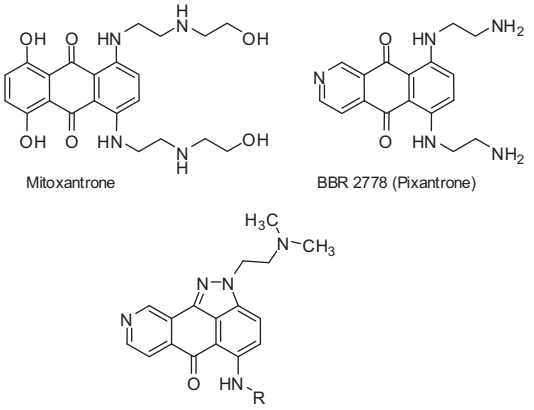

Figure 1. Structures of Mitoxantrone, Pixantrone and novel indazolo[4,3-*gh*]isoquinolinones.

35–**37** by nucleophilic aromatic substitution of chlorine in precursor **11** and subsequent cleavage *t*-butyldiphenylsilyl (TBDPS) protecting group by tetrabutylammonium fluoride (Scheme 3).

O-TBDPS-protected aminohexynol **44** and aminohexenols **45** and **46** were reacted with **11** to give **47**, **48**, and **49** respectively, which were then treated with TBAF to liberate alcohols **24**, **50**, and **51**. Aziridines **26**, **28**, and **29** were prepared from mesylates **25**, **27**, and **52**, which were obtained by reacting mesyl chloride with compounds **24**, **50**, and **51** (Table 2).

Compound **54** was prepared from **11** and *O*-TBDPS-protected aminoethylthioethanol **53** in pyridine. Deprotection was carried out with TBAF in tetrahydrofuran to afford target compound **30** (Scheme 4).

Compound **31** was prepared straightforwardly by nucleophilic aromatic substitution of chlorine of precursor **11** with 2-(2-aminoethylthio)-*N*,*N*-dimethyl-ethanamine **55**[8] (Scheme 5).

The first step of the synthesis of **32** and **33** was the reaction of precursor **11** with side chains **56**[15] and **57**[15] in pyridine to afford compounds **58** and **59**, which were subsequently deprotected by treatment with TBAF to give alcohols **60** and **61**. After mesylation of alcohols **60** and **61**, chlorides **32** and **33** were obtained by treating mesylates **62** and **63**, with lithium chloride in *N*,*N*-DMF (Scheme 6).

In a Grignard reaction *O*-TBDPS-protected butynol **64**[9] was converted into **65** which served as starting material for two different

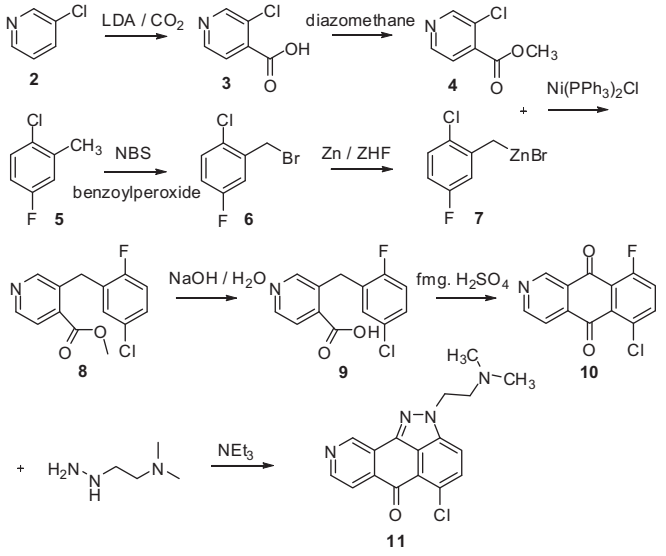

Scheme 1.

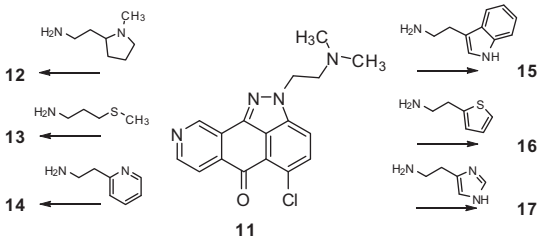

Scheme 2.

Table 1
Structures of novel indazolo[4,3-*gh*]isoquinolinones **12**–**34**

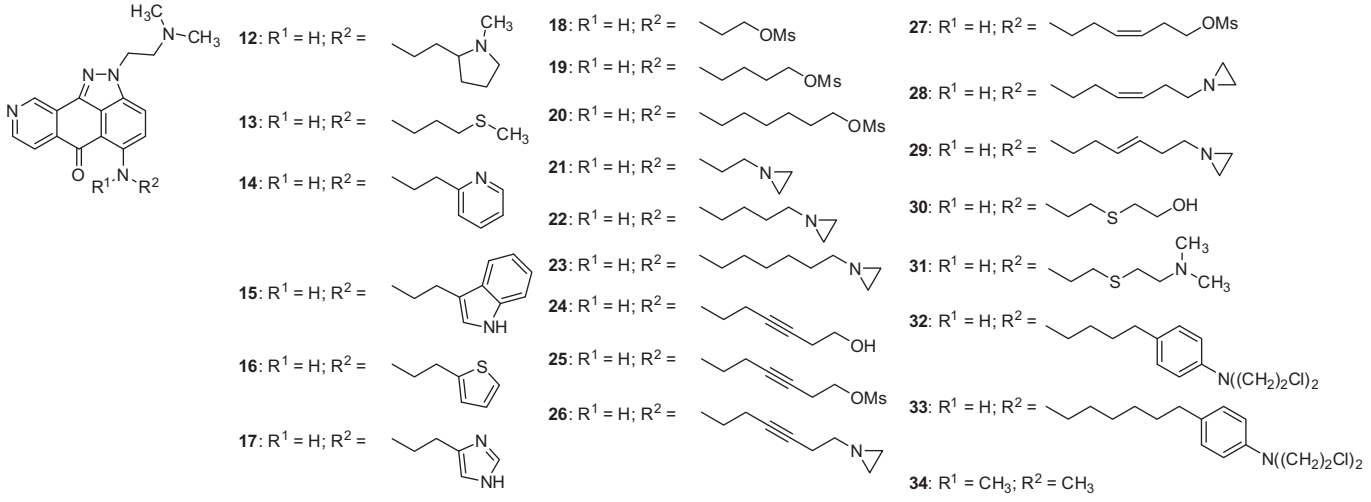

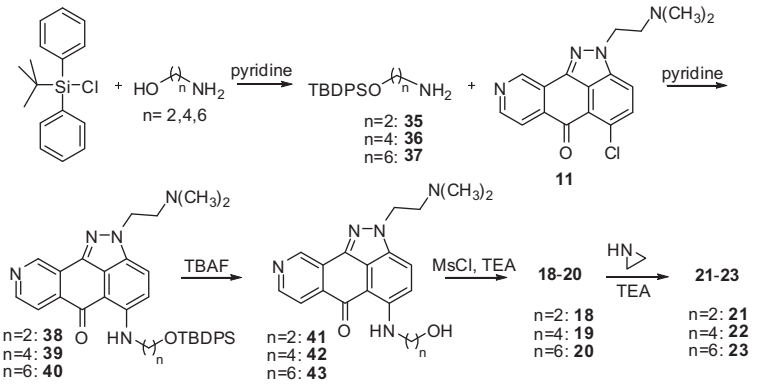

Scheme 3.

Table 2
Synthesis of target compounds **24**–**29**

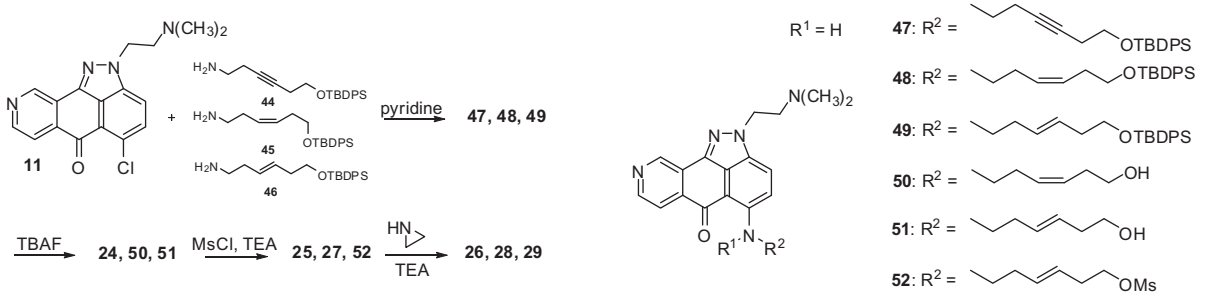

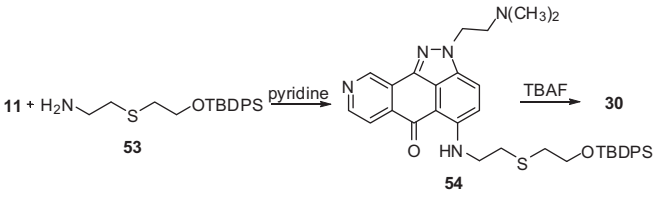

Scheme 4.

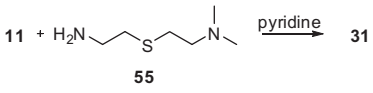

Scheme 5.

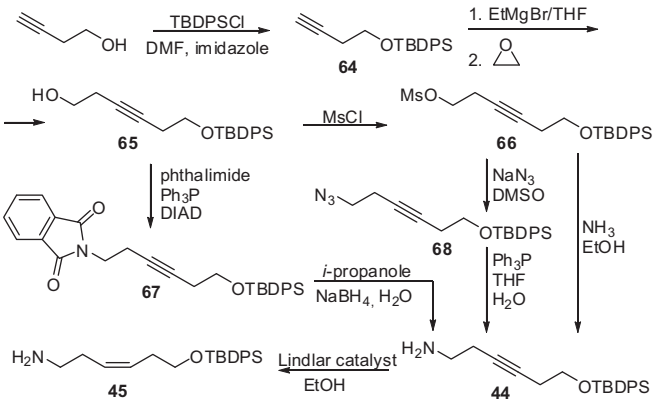

Scheme 7.

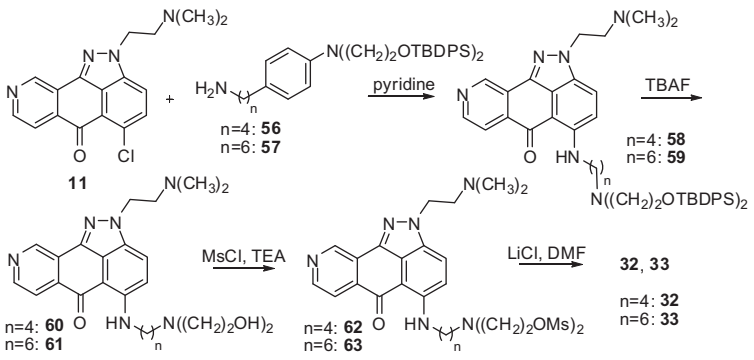

Scheme 6.

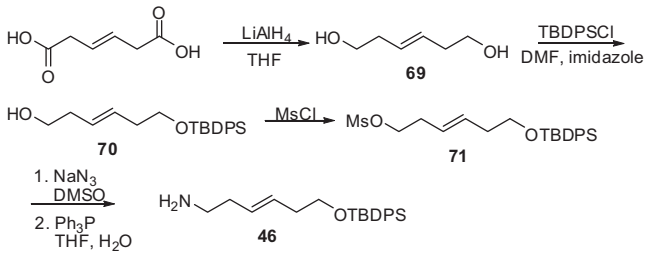

Scheme 8.

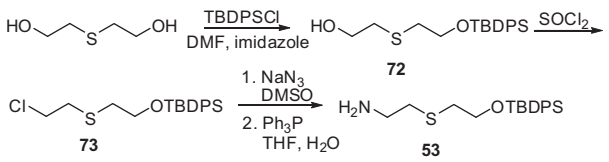

Scheme 9.

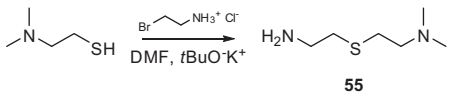

Scheme 10.

pathways to obtain intermediate **44**. In the first pathway amine **44** was introduced by Gabriel synthesis via intermediate **67**. In the second pathway alcohol **65**[10] was reacted with mesyl chloride to give **66**[11] which was either reacted with ammonia in ethanol to give amine **44** directly or with sodium azide and subsequent reduction of **68**–**44**. Finally, *O*-TBDPS-protected (*Z*)-hexenamine **45** was obtained by partial reduction using a lindar catalyst (Scheme 7).

Attempts to prepare **46** from **44** by partial reduction with sodium/liquid ammonia or lithium aluminum hydride failed. Thus, another four-step approach was carried out starting with reduction of 2-butene-1,4-dicarboxylic acid to give diole **69**.[12] This product was mono O-protected by reaction with *t*-butyldiphenylsilyl chloride to afford compound **70**.[13] After mesylation of the remaining hydroxyl group of **70**, the resulting product **71** was reacted with sodium azide in DMSO, followed by reduction of the intermediate azide to afford amine **46** (Scheme 8).

2,2′-Thiodiethanol was mono-protected as *t*-butyldiphenylsilyl ether **72**[14] and subsequently reacted with thionyl chloride to afford compound **73**. Amine **53** was prepared from **73** with sodium azide, followed by treatment with triphenylphosphine and water (Scheme 9).

Amine **55** was straightforwardly prepared by alkylation of 2-(dimethylamino)ethanethiol with 2-bromoethan-amine hydrochloride (Scheme 10).

Compound **74**[16] was prepared from 5-phenylpentanoic acid by nitration in the *para*-position of the phenyl ring. Subsequent esterification led to compound **75**,[17] which was hydrogenated under pressure catalyzed by palladium on carbon to afford amine **77**. Utilizing the same method amine **76** was synthesized from (*E*)-ethyl 3-(4-nitro-phenyl)acrylate. Following reaction steps were carried out in the same manner for both amines **76**[18] and **77**[18] starting with dihydroxyethylation of the nitrogen atoms with ethylenoxide. Both hydroxyl groups of reaction products **78**[19] and **79**[19] were then protected (**80**, **81**)[20] with *t*-butyldiphenylsilyl chloride and the ester moieties reduced to alcohols **82** and **83**. Mesylation of the hydroxyl groups of alcohols **82**[20] and **83**[20] and immediate treatment with lithium bromide gave bromides **84**[21] and **85**[21] which upon treatment with tetraethylammounium cyanide were converted into nitriles **86**[22] and **87**.[22] Final reduction of the nitrile moieties with lithium aluminum hydride afforded the desired amine products **56** and **57** (Scheme 11).

Indazolo[4,3-*gh*]isoquinolinones **12**–**34** were analysed regarding their cytotoxic/antiproliferative activity against different cancer cell lines, namely KB/HeLa (cervical carcinoma), SKOV-3 (ovarian carcinoma), SF-268 (CNS, glioma), NCI-H460 (non-small cell lung carcinoma (NSCLC)), and of RKOp27 (colon adenocarcinoma).[23] The concentration of the compound that inhibits 50% (EC_{50}) of cellular viabilty after 48 h was calculated by nonlinear regression (GraphPad Prism™) using the data of at least two independent cytotoxicity assays.[24] Results of the cytotoxicity assays are shown in detail in Table 3.

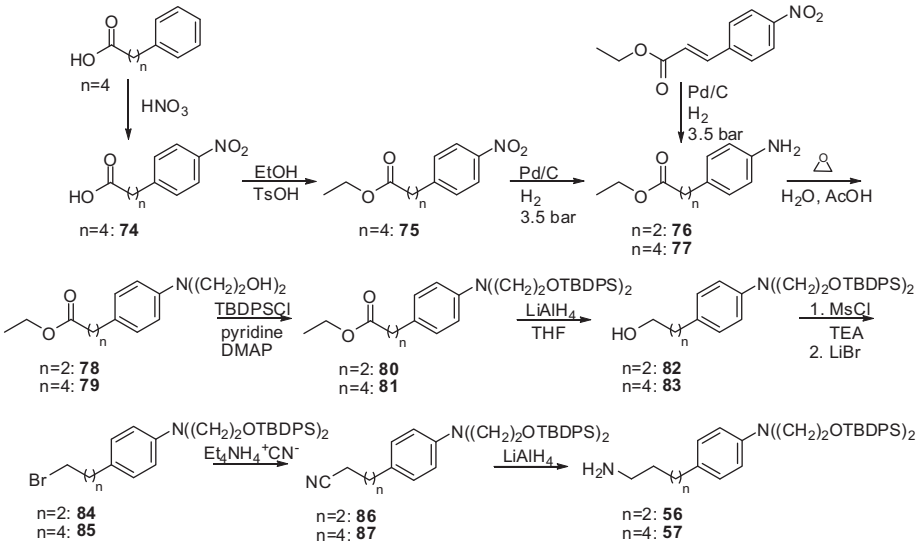

Scheme 11.

Table 3
In vitro cytotoxicity of compounds **12**–**34** towards different cell lines

Cells (origin)/compound	EC_{50}[a] (μM)					
	KB/HeLa (cervix)	SKOV-3 (ovarian)	SF-268 (CNS)	NCI-H460[b] (NSCLC)	RKOp27 (colon)	RKOp27IND (colon)
12	Not tested	0.36 ± 0.00 (2)	Not tested	0.16 ± 0.01 (2)	0.37	0.46
13	Not tested	1.36 ± 0.33 (2)	Not tested	0.68 ± 0.05 (2)	2.94	4.76[d]
14	Not tested	1.41 ± 0.30 (2)	Not tested	0.99 ± 0.12 (2)	2.68	3.77
15	Not tested	1.52 ± 0.11 (2)	Not tested	1.32 ± 0.02 (2)	1.33	1.51
16	Not tested	3.22 ± 0.22 (2)[d]	Not tested	1.47 ± 0.12 (2)	3.12[d]	4.84[d]
17	Not tested	1.65 ± 0.18 (2)	Not tested	3.02 ± 0.02 (2)[d]	1.33	4.81[d]
18	0.15	0.55	0.39	0.25	0.17	1.83
19	3.17[d]	No inhib.[c]	No inhib.[c]	1.07	1.18	No inhib.[c]
20	1.67	3.61[d]	1.37	0.82	0.51	1.93
21	0.07	0.39	0.69	0.08	0.08	1.05
22	0.08	0.53	0.42	0.07	1.00	1.02
23	0.34	0.77	0.76	0.20	0.13	1.28
24	1.39	1.21 ± 0.00 (2)	3.45[d]	0.68 ± 0.14 (2)	1.63	3.23[d]
25	0.39	0.73 ± 0.07 (2)	0.75	0.411 ± 0.08 (2)	0.47	0.98
26	0.14	0.31 ± 0.10 (2)	0.24	0.06 ± 0.00 (2)	0.07	0.35
27	0.75	5.38	3.07[d]	2.18	0.63	2.61
28	0.43 ± 0.21 (3)	1.77 ± 1.11 (3)	1.71 ± 0.53 (3)	0.59 ± 0.37 (3)	0.29 ± 0.15 (3)	1.20 ± 0.49
29	1.22	3.22[d]	2.99	0.69 ± 0.10 (2)	0.72	2.78
30	0.96	0.40 ± 0.00 (2)	0.66	0.15 ± 0.03 (2)	0.55	1.06
31	0.75	0.70 ± 0.00 (2)	2.37	0.31 ± 0.05 (2)	0.92	1.79
32	2.47	No inhib.[c]	4.17[d]	3.76[d]	1.19	1.63
33	No inhib.[c]	No inhib.[c]	No inhib.[c]	No inhib.[c]	No inhib.[c]	No inhib.[c]
34	2.19	2.08 ± 0.30 (2)	1.34	0.77 ± 0.07 (2)	2.63	3.06[d]
Mitoxantrone	0.36 ± 0.14 (5)	0.12 ± 0.04 (3)	0.32 ± 0.21 (3)	0.12 ± 0.01 (3)	0.09 ± 0.01 (3)	0.76 ± 0.20

[a] EC_{50} values determined in replicates are given as mean values ± standard deviation with number of replicates given in round brackets.
[b] EC_{50}(NCI-H460) denotes the activity for NCI-H460 cell line, which is employed to compare compound activities.
[c] No inhib. = no inhibition, that is <30% inhibition in the highest concentration (3.16 μM) during EC_{50} determination.
[d] 'Moderate' activity describes compound activity, that showed at least 30% inhibition in the highest concentration (3.16 μM) during EC_{50} determination, but since a full dose–response curve is not available, compound activity has been described as EC_{50} >3 μM.

Table 4
DNA intercalation for selected compounds demonstrated by the shift of the most blue shifted respective peaks

Compound	DNA—intercalation
22	508 → 514 nm
24	505 → 512 nm
26	505 → 512 nm
30	505 → 513 nm
34	491 → 499 nm
12	502 → 510 nm
23	509 → 515 nm
15	No intercalation
Acridine	492 → 502 nm
Mitoxantrone	662 → 681 nm

A first comparison between the tested indazolo isoquinolinones and reference compound Mitoxantrone reveals excellent antiproliferative activity. Within this report, EC_{50}(NCI-H460) activity values will be used to compare compounds. Based on this activities, an improvement by a factor of two with regard to Mitoxantrone is observed for **26** and **22** (EC_{50}(NCI-H460): 0.062 and 0.071 μM vs 0.122 μM). Compound **30**, **12** and **23** show a similar antiproliferative activity (EC_{50}(NCI-H460): 0.151 μM, 0.159 μM and 0.195 μM, respectively).

Due to the similarity of the indazolo isoquinolinones and reference compound Mitoxantrone, DNA intercalation[25] as a possible mode of action was evaluated for a set of selected compounds.

Using Acridine and Mitoxantrone as positive controls, the tested indazolo isoquinolinones clearly show DNA intercalation (see Table 4). Mitoxantrone moves the most blue shifted peak (i.e., at 662 nm) for 19 nm. The tested indazolo isoquinolinones consistently shift their respective peaks for 6–8 nm (shown in Fig. 2).

Comparison of the activities of indazolo isoquinolinones against RKOp27 with or without p27 induced cell cycle arrest suggest, that progression through cell cycle might be required for the mode of action for some, but not all compounds analysed. In order to examine the compound effects on cell cycle by FACS analysis, exponentially dividing KB/HeLa cells were treated with different concentrations of selected compounds for 48 h and compared to untreated controls.[26]

Results from these cell cycle studies are rather inhomogeneous. This is exemplified by compounds **26** (χ-hexinyl spacer), **23** (hexane spacer, 0.195 μM), **28** (*cis* χ-hexene spacer, 0.594 μM) and **29** (*trans* χ-hexene spacer, 0.691 μM) as depicted in Table 5.

Aziridine **26**, showing the best NCI-H460 activity within the series, is not at all inducing cell cycle arrest in KB/HeLa cells, while the other C6 spaced aziridines do so with single digit micromolar EC_{50} values.

Moreover, inverse dose-dependent S-phase arrest is observed for compounds **23**, **28** (see Fig. 3) and **29**, which is a rarely observed dose depency feature.

Further experiments will be necessary to explain these unusual effects.

In conclusion, a series of indazolo[4,3-*gh*]isoquinolinones were synthesized and tested for antiproliferative activity against at least four cancer cell lines. Compared to reference compound Mitoxantrone, aziridine **23** turned out to show an increase in activity by a factor of 2.

Cell cycle arrest studies gave complex results, including an induction of S-phase arrest with an inversed dose dependency.

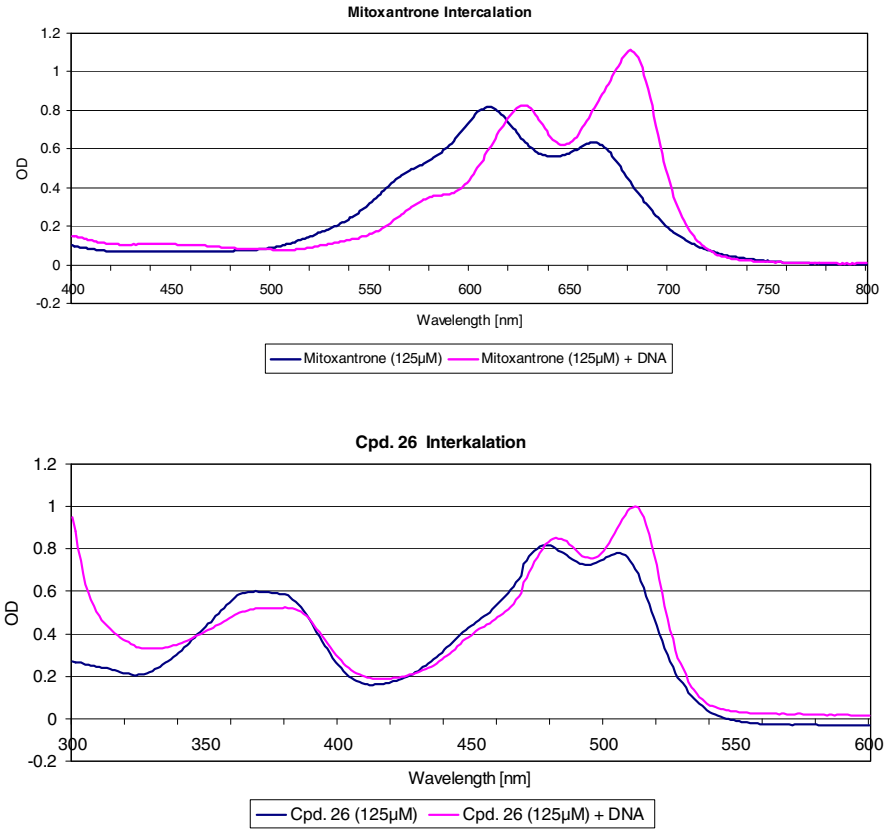

Figure 2. UV spectra showing DNA intercalation of reference compound Mitoxantrone and aziridine **26**.

Table 5
Cell cycle arrest results for aziridines **23**, **26**, **28** and **29**

Compound	Cell cycle
26	No cell cycle arrest
23	Increase of S-Phase below 4 µM with inverse dose dependency
28	Increase of S-Phase below 6 µM with inverse dose dependency
29	Increase of S-Phase below 7 µM with inverse dose dependency

Supplementary data

Supplementary data associated with this article can be found, in the online version, at http://dx.doi.org/10.1016/j.bmcl.2013.01.022.

References and notes

1. Vuimo, T. A.; Kulikova, E. V.; Sinauridze, E. I.; Yurkevich, A. M.; Kravchenko, S. K.; Ataullakhanov, F. I. In *New Research on Biotechnology and Medicine*; Egorov, A. M., Zaikov, G., Eds.; Nova Science Publishers: New York, 2006; p 87.
2. Pettengell, R.; Coiffier, B.; Narayanan, G.; de Men-doza, F. H.; Digumarti, R.; Gomez, H.; Zinzani, P. L.; Schiller, G.; Rizzieri, D.; Boland, G.; Cernohous, P.; Wang, L.; Kuepfer, C.; Gorbatchevsky, I.; Singer, J. W. *Lancet Oncol.* **2012**, *13*, 696.
3. Krapcho, A. P.; Gallagher, C. E.; Hammach, A.; Hacker, M. P.; Menta, E.; Oliva, A.; Di Domenico, R.; Da Re, G.; Lotto, A.; Spinelli, S. *J. Heterocycl. Chem.* **1998**, *35*, 895.
4. Tomillero, A.; Moral, M. A. *Methods Find. Exp. Clin. Pharmacol.* **2009**, *31*, 661.
5. Shanab, K.; Schirmer, E.; Knafl, H.; Wulz, E.; Holzer, W.; Spreitzer, H.; Schmidt, P.; Aicher, B.; Mueller, G.; Guenther, E. *Bioorg. Med. Chem. Lett.* **2010**, *20*, 3950.
6. Pongprom, N.; Bachitsch, H.; Bauchinger, A.; Ettefagh, H.; Haider, T.; Hofer, M.; Knafl, H.; Slanz, R.; Waismeyer, M.; Wieser, F.; Spreitzer, H. *Monatsh. Chem.* **2010**, *141*, 53.
7. Shanab, K.; Pongprom, N.; Wulz, E.; Holzer, W.; Spreitzer, H.; Schmidt, P.; Aicher, B.; Müller, G.; Günther, E. *Bioorg. Med. Chem. Lett.* **2007**, *17*, 6091.
8. Ohno, M.; Miyamoto, M.; Hoshi, K.; Takeda, T.; Yamada, N.; Ohtake, A. *J. Med. Chem.* **2005**, *48*, 5279.
9. Labelle, M.; Falgueyret, J.-P.; Riendeau, D.; Rokach, J. *Tetrahedron* **1990**, *46*, 6301.

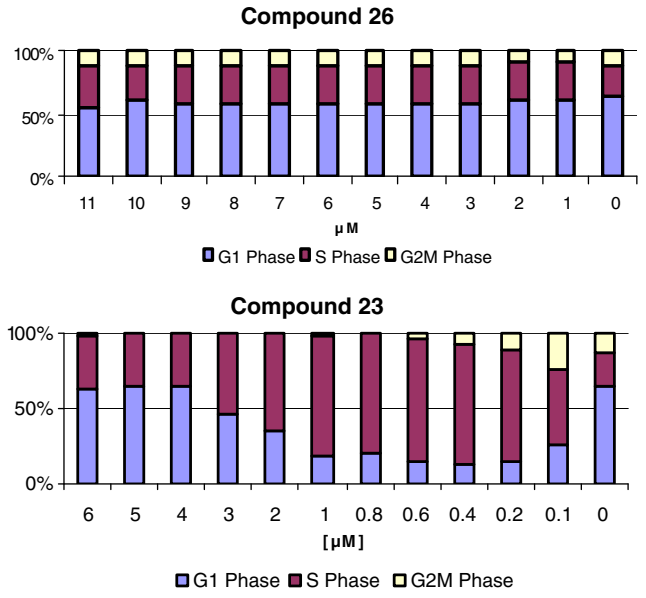

Figure 3. Cell cycle arrest results for aziridines **26** and **23**. While no cell cycle arrest is observed by treatment with up to 11 µM of aziridine **26**, compound **23** induces S-phase arrest with an inverse-shaped dose–response, peaking between 1 and 0.2 µM, and flanked by transition to normal cell cycle distribution at concentrations above and below this concentration range. Similar data are shown in the supporting materials section.

10. Collins, C. J.; Hanack, M.; Stutz, H.; Auchter, G.; Schoberth, W. *J. Org. Chem.* **1983**, *48*, 5260.
11. Delorme, D.; Girard, Y.; Rokach, J. *J. Org. Chem.* **1989**, *54*, 3635.
12. Eya, B. K.; Otsuka, T.; Kubo, I.; Wood, D. L. *Tetrahedron* **1990**, *46*, 2695.
13. Braddock, D. C.; Bhuva, R.; Millan, D. S.; Perez-Fuertes, Y.; Roberts, C. A.; Sheppard, R. N.; Solanki, S.; Stokes, E. S. E.; White, A. J. P. *Org. Lett.* **2007**, *9*, 445.

14. Zacharie, B.; Gagnon; Attardo, G.; Connolly, T. P.; St-Denis, Y.; Penney, C. L. *J. Med. Chem.* **1997**, *40*, 2883.
15. Abd El Samii, Z. K. M.; Al Ashmaney, M. J.; Mellor, J. M. *J. Chem Soc., Perkin Trans. 1* **1988**, 2517.
16. Denny, W. A.; Cain, B. F. *J. Med. Chem.* **1978**, *21*, 430.
17. Becker, H. G. O.; Berger, W.; Domschke G. Organikum, 21. Auflage, Deutscher Verlag der Wissenschaften, Weinheim, 2001. p. 475.
18. Street, L. J.; Baker, R.; Castro, J.; Chambers, M. S.; Guiblin, A. R.; Hobbs, S. C.; Matassa, V. G.; Reeve, A. J.; Beer, M. S. *J. Med. Chem.* **1993**, *36*, 1529.
19. Kupczyk-Subotkowska, L.; Siahaan, T. J.; Basile, A. S.; Friedman, H. S.; Higgins, P. E.; Song, D.; Gallo, J. M. *J. Med. Chem.* **1997**, *40*, 1726.
20. Pichler, A. Ph.D. Thesis, University of Vienna, 1996.
21. Wissner, A.; Carroll, M. L.; Johnson, B. D.; Kerwar, S. S.; Pickett, W. C.; Schaub, R. E.; Torley, L. W.; Trova, M. P.; Kohler, C. A. *J. Med. Chem.* **1992**, *35*, 4779.
22. Kobler, H.; Schuster, K. H.; Simchen, G. *Liebigs Ann. Chem.* **1978**, 1946.
23. Schmidt, M.; Lu, Y.; Liu, B.; Fang, M.; Mendelsohn, J.; Fan, Z. *Oncogene* **2000**, *19*, 2423.
24. Assessment of cytotoxic/antiproliferative activity was conducted with five diverse tumor cell lines, in which inducible expression of the cell cycle inhibitor p27Kip1 leads to cell arrest (see Ref. [23]).
Measurement of the cellular cytotoxic/antiproliferative activity is based on the dye Resazurin (Sigma, cat. no. R7017), which exhibits fluorescence change in the appropriate oxidation-reduction range relating to cellular metabolic reduction (Nociari et al., *J. Immunol. Methods* **1998**, *213*, 157) yielding a fluorescence signal at 590 nm. The increase of fluorescence at 590 nM is an indicator of cellular viability/cell number.
The cells were seeded in the respective growth medium recommended by the supplier (media and reagents purchased from Gibco-BRL) in 125 μl per 96 well and were grown for 24 h at 37 °C/5% CO_2. Cell numbers were adapted for each cell line to generate signals in the linear detection range under the experimental conditions applied. After 45 h of compound incubation at 37 °C/5% CO_2 15 μl of the Resazurin detection reagent (0.2 mg/mL in DPBS (Gibco, 14190), steril filtered) was added for additional 3 h and after a total of 48 h of compound incubation cellular metabolic activity was quantified by measurement of fluorescence at 590 nm. Non-treated cells and blank controls w/o cells were set as reference values.
MS EXCEL was used for formating and analysis of data. All data were calculated as % efficacy compared to the mean of the respective negative (non-treated cells) and positive control wells (blank) on each assay plate. EC_{50} values (Table 3) were calculated by using non-linear regression software GraphPad Prism.
25. Stock solution of reference and test compounds up to 5 mM concentration in 5% (v:v) DMSO or methanol were prepared. The compound solution was diluted stepwise in reaction buffer (5 mM NaH2PO4, 5 mM Na2HPO4, 70 mM NaCl, pH7) and a compound concentration resulting in absorbance [Abs max] of approx. 1–2 between 230 and 600 nm using a Spectramax 190 plus reader (Molecular Devices, Sunnyvale, CA) was determined. Finally, curves for these compound concentrations were compared with or without 2 mg/ml (w:v) calf thymus DNA (Sigma–Aldrich Corp., St. Louis, MO).
26. Flow cytometry analysis was done at FACSCalibur™ cytometer (Becton Dickinson, Heidelberg, GER). For cell cycle analysis, KB/HeLa cells (ATCC CCL17) were exposed to test compounds for 24 h @ 37 °C. Cell preparation was done with CycleTEST™ PLUS kit. The number of cells in G_2/M phase was calculated by cell cycle analysis software (Mod Fit LT; VERITY) and EC_{50}-values were calculated by nonlinear regression.